ADVANCED MATERIALS

Supporting Information

for *Adv. Mater.*, DOI: 10.1002/adma.201405438

Self-Fueled Biomimetic Liquid Metal Mollusk

*Jie Zhang, Youyou Yao, Lei Sheng, and Jing Liu**

SUPPLEMENTARY INFORMATION

Self-Fueled Biomimetic Liquid Metal Mollusk

Jie Zhang[1], Youyou Yao[1], Lei Sheng[1], Jing Liu[1,2*]

1. Department of Biomedical Engineering, School of Medicine, Tsinghua University, Beijing 100084, China

2. Technical Institute of Physics and Chemistry, Chinese Academy of Sciences, Beijing 100190, China

*E-mail Address: jliubme@tsinghua.edu.cn

SI Appendix 1: Design and fabrication of typical channel structures

To investigate the basic characteristics of the self-propelled locomotion of the liquid metal motor in different types of trajectories through feeding aluminum as fuels, we have designed and manufactured several channels with representative shapes elaborately, either straight or somewhat irregularly structured. There are totally four types of open-top channels that we have conducted experiments in: 1. Circular channel; 2. U-shaped channel; 3. Straight channel; and 4. Zigzag channel. Supplementary **Figure S1a** depicts the designed shapes and sizes of these channels, and Supplementary **Figure S1b** shows the actually fabricated channels. Supplementary **Figure S2** and **Movies S1-S5** demonstrate the actual running of the liquid metal motor in such channels where it is found that the motor conforms well to the wall, no matter what its shape, structure or surface roughness is. This amazing behavior reveals the pretty high adaptability of the liquid metal mollusk when facing various situations.

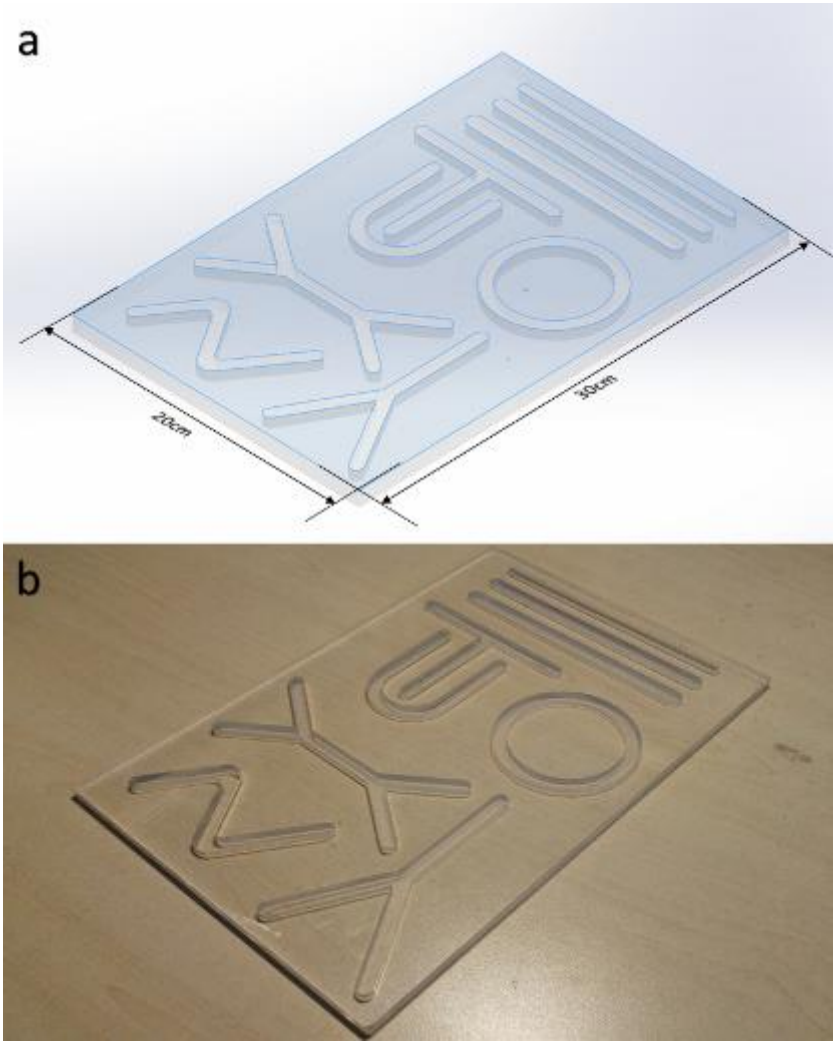

Figure S1. The size of the substrate and the shapes of several representative fabricated channels. **(a)** The figure designed by the software SolidWorks 2012. **(b)** The manufactured entity by PMMA material.

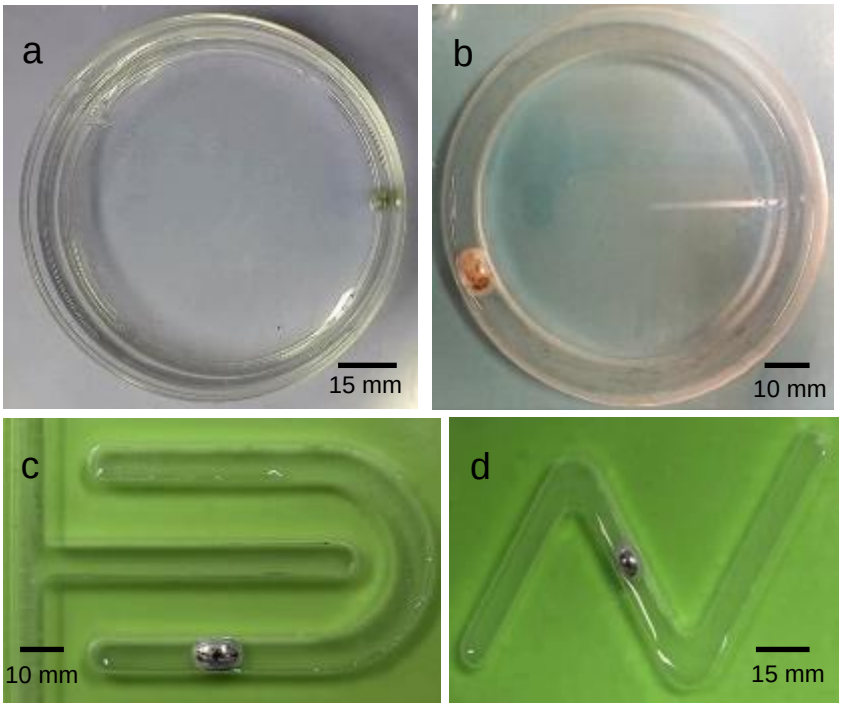

Figure S2. Schematic for the running of a liquid metal motor in different channel structures. **(a)** Free space in Petri dish. **(b)** Circular channel. **(c)** Hybrid channel with straight and semi-circular structures. **(d)** Zigzag channel.

SI Appendix 2: Locomotion of a liquid metal motor in free space of a Petri dish

As has been clarified by the present work, the locomotion of the liquid metal motor is actuated in principle by the EGaIn-Al galvanic cell reaction. To perform the experimental tests, we use tweezers to pick up a small aluminum (Al) flake and attach it to the liquid metal EGaIn object, which looks just like feeding the mollusk. Both Al and liquid metal object are immersed in 0.25 mol/L NaOH solution in a Petri dish. After approximately one minutes, the contacting site between Al and EGaIn liquid metal starts galvanic cell reaction with bubbles generated under observation of a digital microscope. Al chemically reacts with NaOH solution which can be denoted by the following equation as:

$$2Al+2NaOH+2H_2O=2NaAlO_2+3H_2\uparrow \quad (1)$$

This reaction can be observed that when Al is immersed in NaOH solution, small bubbles are slowly generated and depart from the surface of aluminum. When Al starts to attach to the EGaIn droplet, the liquid metal droplet slightly flicks away due to its high surface tension. After several repeats of the attachment, Al and liquid metal droplet merge together and the reaction rate is

accelerated with lots of bubbles emerging from the solution. Simultaneously, the liquid metal motor starts to self-rotate on the lateral, which induces a flow field in the aqueous solution. The direction of the lateral motion is correlated to the position of Al-liquid metal reaction point, and such swirling behavior can be clearly indicated by the accompanied floating and moving bubbles.

When the local self-rotation of the liquid metal droplet launches, the droplet starts to move along the wall of the Petri dish (**Figure S3**), working similar to a mollusk. It looks here the dish wall always serves as a supporting track for positioning the running metal (**Figure S3a, b, c, d**; and **Movie S1**). When stirred by glass capillary, such motor may change its locomotion direction temporarily but still keeps running along with the wall of the Petri dish autonomously after the removal of the disturbance. With different volumes of the liquid metal and aluminum fuel, various running speed and lasting time can be achieved. This can assist future design of a practical machine in the coming time.

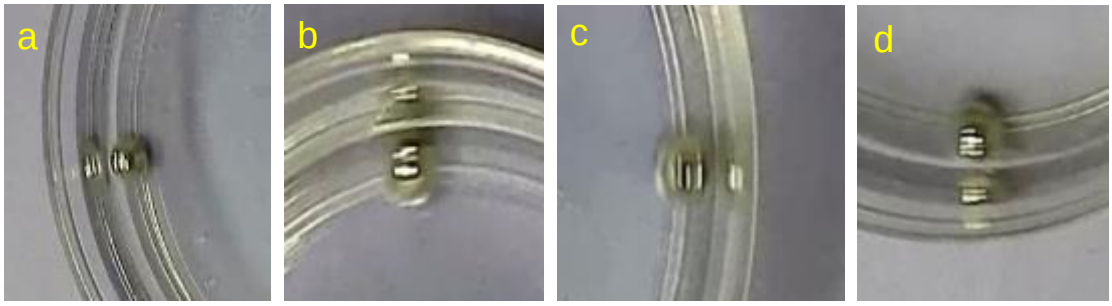

Figure S3. Schematic for four positions of liquid metal motor running along the wall of the Petri dish. **(a)** Left hand side wall. **(b)** Upper wall. **(c)** Right hand side wall. **(d)** Bottom wall.

SI Appendix 3: Adaptability of liquid metal mollusk to various surface profiles and structures of PMMA channels

Through repeated experiments, we find that the liquid metal motor owns rather outstanding adaptability to various channel profiles, either smooth or rough. The capability of this soft machine appears much superior compared with rigid robots and deserves to be developed as practical machines in the near future. To characterize the surface property of the channels, the white-light interference profilometer is implemented to measure the surface roughness of the channels. The results were depicted in **Figure S4**. It is found that the fabricated channel has in fact intrinsically a relatively rough surface which is not as smooth as a Petri dish. For a rigid machine,

it may be incapable of moving in such irregularly structured channel. But for the current liquid metal motor, it can easily overcome the barriers owing to its entirely soft property and extremely low rolling friction. As is measured, the average roughness of PMMA channel is about Sa=2 um, and the straight section appears relatively smoother than that of the curved section of the channel. One surprising fact is that, the liquid metal motor runs smoothly throughout all these channels, even some surfaces of which are rather rough. Except for adapting to the surface property, the current liquid metal motor can also very well adapt to various structured channels, either straight or irregular (**Movies S2, S3, S4, S5**). As is shown in the hybrid channel structure of **Figure S5** and zigzag channel in F**igure S6**, when moving into different places with varied cross sectional channel, the liquid metal motor flexibly modifies its configuration so as to move smoothly across the corresponding site. The various ratios among these transient shapes or cross sectional areas can be rather large, which is hard to achieve otherwise by an ordinary rigid machine. This again demonstrates the unusual capability for the new biomimetic machine. Presented in **Figure S7**, it depicts the transient motion velocity and displacement of the liquid metal mollusk when crawling within the zigzag channel. Clearly, due to the relatively large volume of the motor and the irregularly sized narrow channel, the moving speed here is much slower than that in the former case. Another reason of the slower velocity is that the trip is somewhat more challenging. Further, it is also very interesting to observe that, when the motor reaches the corner, it stays there for a short break without evident movement. Later soon, it resumes its motion activity again along the zigzag channel.

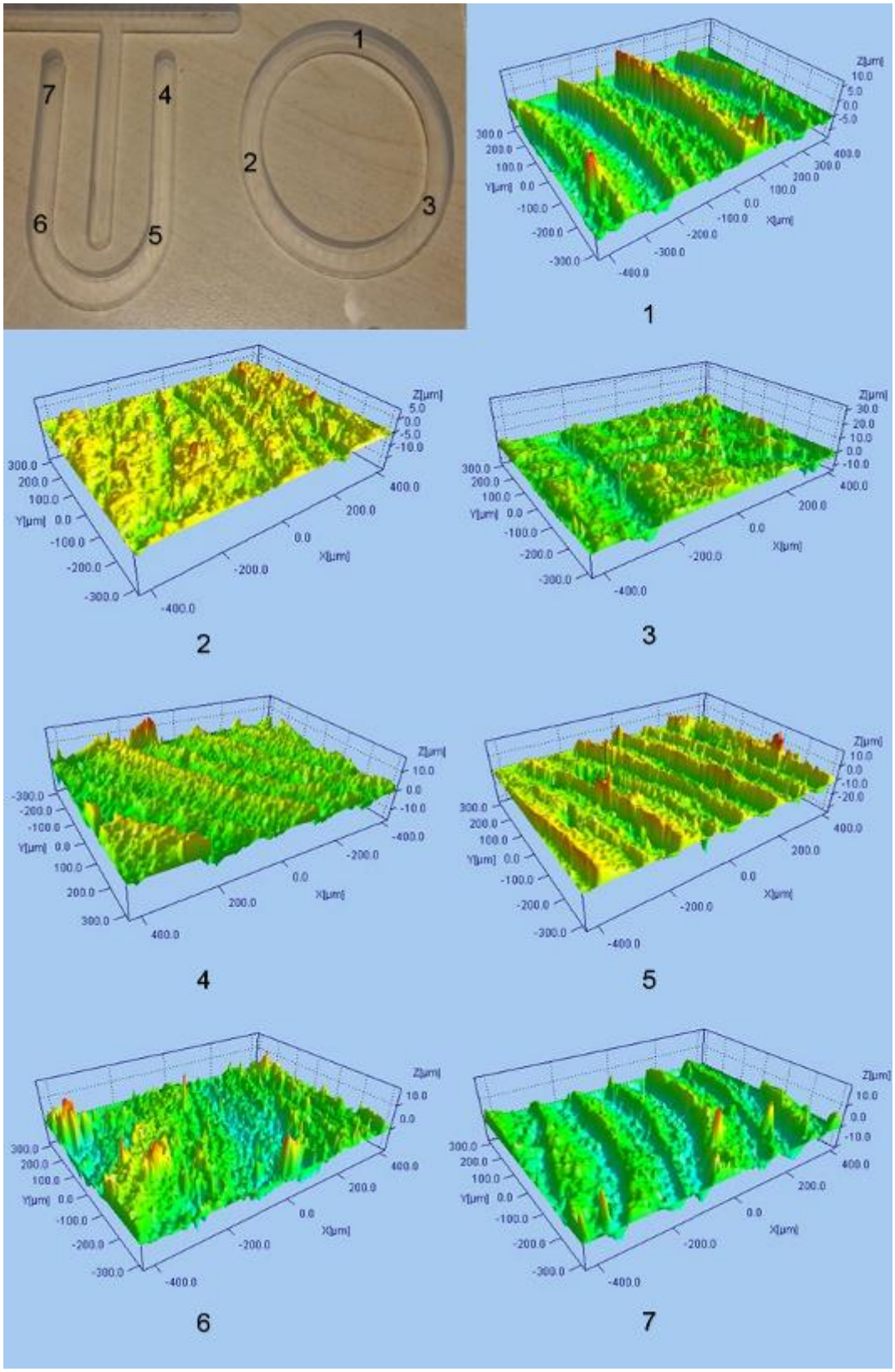

Figure S4. The fabricated channel (upper left) and surface roughness of various sites along the PMMA channels. Here, seven sites from 1 to 7 are marked to measure the surface characteristics. Pseudo-color is used to display surface topography more intuitionally.

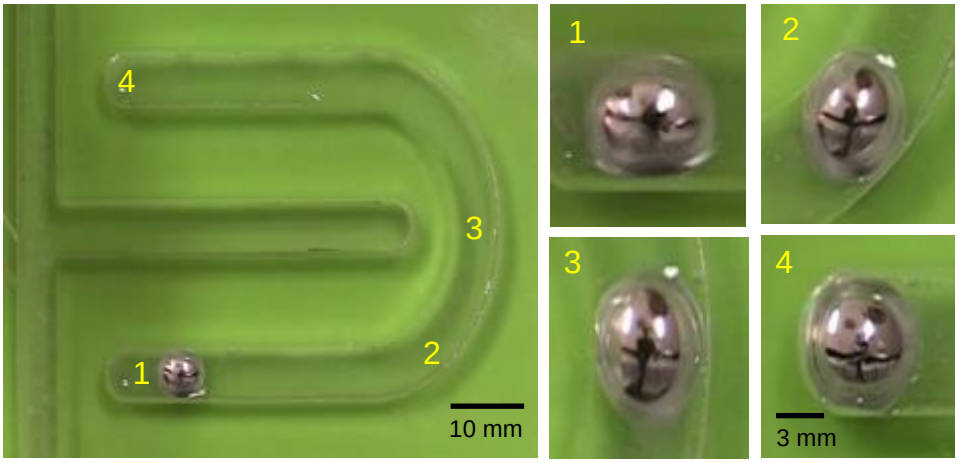

Figure S5. Running of liquid metal motor and its respective configurations at four positions inside the hybrid structured channel. Here, 1, 2, 3 and 4 refer to four positions that liquid metal motor is moving onto.

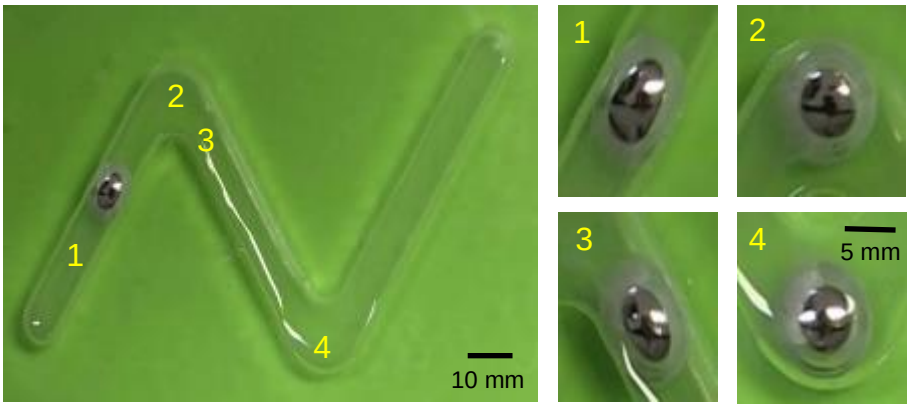

Figure S6. Running of liquid metal motor and its respective configurations at four positions inside the zigzag channel. Here, 1, 2, 3 and 4 refer to four positions that liquid metal motor moves into.

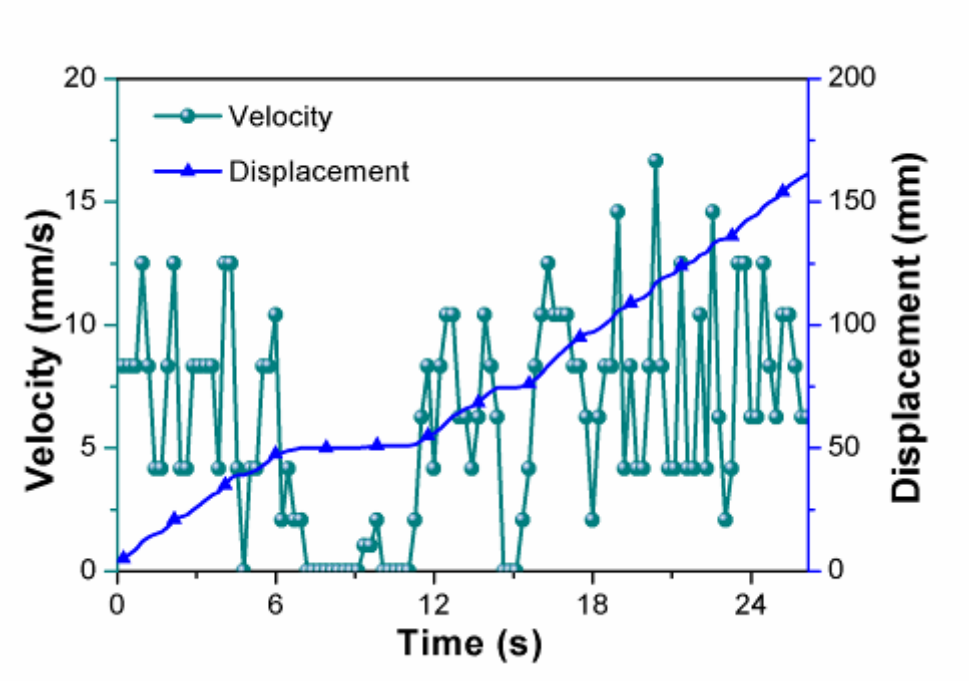

Figure S7. Moving velocity and displacement of liquid metal mollusk across the zigzag structured channel. The sites where the velocity drops to zero are the corners for the motor to adapt itself to the changeable channel.

SI Appendix 4: The stop of the autonomous movement

It looks the stop of the movement is not likely due to the depletion of Al. As was observed, after the motor stops moving, bubbles are still emerging from the surface of the liquid metal, and the reaction area takes up a larger surface, indicating the Al is not depleted. This mainly results from that the amalgamation of Al by the liquid metal renders the intact Al to form into lots of small fragments [1], and these fragments cover a larger surface of liquid metal, which breaks the asymmetry. Besides, as time goes on, bubbles accumulate on the surface of the metal and in the channel, which hinders the movement as well. The surface of the liquid metal at different times can be found as shown in **Figure S8**.

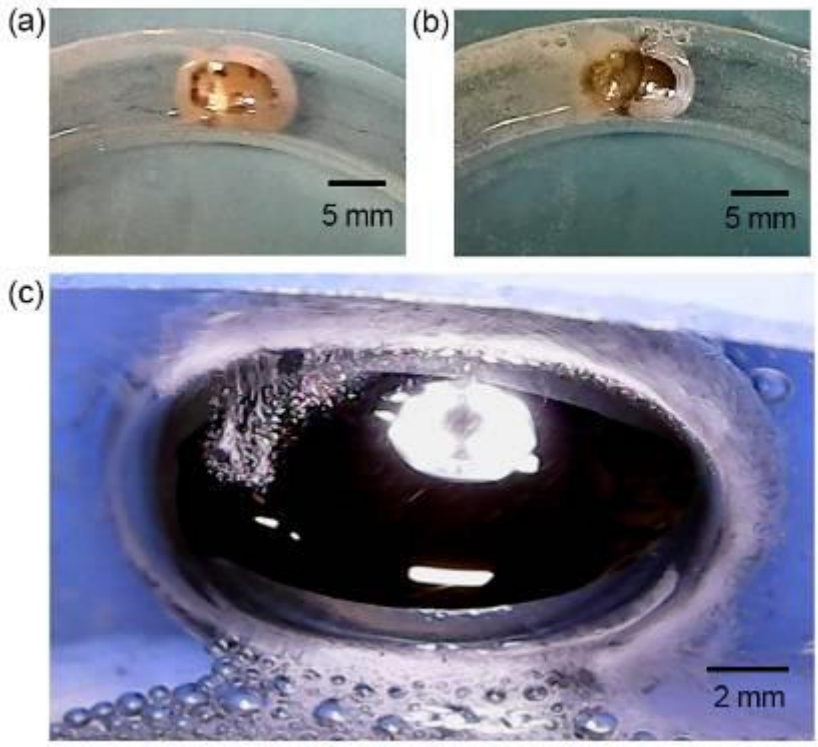

Figure S8. The surface of the liquid metal at different times. The 160-μL EGaIn motor moves in a circular open-top channel containing 0.25 mol/L NaOH solution. (a) The motor moves at 10 minutes. (b) The motor moves at 52 minutes. (c) The motor stops moving at 70 minutes.

SI Appendix 5: Nearby flow field of liquid metal motor in the reaction.

For more details on the running mechanism of the current mollusk machine, a digital microscope is employed to observe the nearby flow around the liquid metal induced by the lateral self-rotation of the motor and the bubble generation when the metal droplet is fixed at a certain site (**Movies S9** and **S10**). With the indication of the bubbles, the velocities and the flow direction of the aqueous solution in different area of flow field are clearly demonstrated, as is shown in **Figure S9**. The solution along both the front (**Figure S9a**) and rear (**Figure S9b**) of the liquid metal motor flows anticlockwise. And at further distance away from the liquid metal, the flow rate slows down gradually. Additionally, some bubbles depart from the rear of the liquid metal motor where the Al is attached.

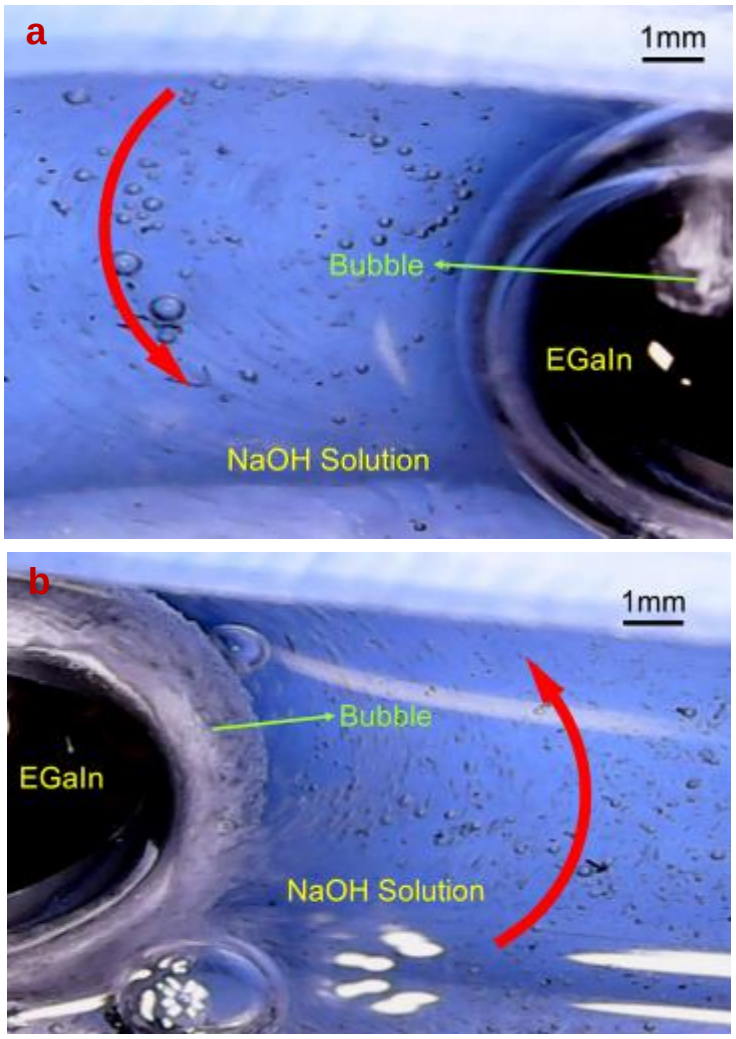

Figure S9. The flow field of the solution around the liquid metal motor displayed by the trajectory of the bubble departure. **(a)** The flow field on the left hand side of the liquid metal. **(b)** The flow field on the right hand side of the liquid metal.

SI Appendix 6: The resistance from the solution to overcome for the actuation

It is inappropriate to use Stokes law to characterize the driving force for the droplet in the Pertri dish to move since the Reynolds number for the current flow ranges from 240 to 290. The real resistance is larger than the calculation based on Stokes law. Theoretically, the resistance F for a sphere moving in fluid can be expressed as follows:

$$F = C_D \frac{1}{2} \rho v^2 A \quad (1)$$

where C_D is resistance factor, ρ is density of the fluid, v the velocity of the sphere relative to the

distant fluid, and A is the meeting area of flowing, which equals to πr^2 (r is the radius of the sphere) for a sphere. From Equation 1, one can get the resistance factor:

$$C_D = \frac{F}{(\rho v^2/2)\ \pi r^2} \tag{2}$$

For a sphere moving in the fluid, the Reynolds number Re is calculated as follows:

$$Re = \frac{2r\rho v}{\mu} \tag{3}$$

where r is the radius of the sphere, ρ is density of the fluid, v is the velocity of the sphere relative to the distant fluid, and μ is the viscosity of the fluid. Under the condition that $Re<1$, according to the Stokes law, the resistance is:

$$F = 6\pi\mu r v \tag{4}$$

According to Equation 2, Equation 3 and Equation 4, the resistance factor is expressed as follows:

$$C_D = \frac{24}{Re} \tag{5}$$

However, when $Re>1$, the resistance obtained based on Equation 4 is smaller than the real resistance. There is an empirical formula by fitting to experimental data to calculate the resistance factor [2], i.e.

$$C_D = \frac{24}{Re} + \frac{6}{1+\sqrt{Re}} + 0.4, \qquad 0 \le Re \le 2\times 10^5 \tag{6}$$

The maximum error calculated by Equation 6 is 10%. The Reynolds number is much less than $2*10^5$, thus Equation 6 is applicable for the calculation of the resistance. Based on Equation 1, Equation 3 and Equation 6, which are all applicable when $Re>1$, we can get that the resistance for a sphere is as follows:

$$F = 6\pi\mu v r + \rho\pi r^2 v^2 \left(\frac{3}{1+\sqrt{\rho v r/\mu}} + 0.2\right) \tag{7}$$

Comparing Equation 7 with Equation 4, one can get that when $Re>1$, using Equation 4 to estimate the resistance induces that the calculated result deviated from the fact, and the resistance calculated from Equation 4 is smaller than that based on Equation 7.

Therefore, from Equation 4 and Equation 7, when the motor size scales from nano-/micrometers to milli-/centimeters, the resistance for the motor to overcome increases 3-6 orders under no consideration of velocity. However, as the reported velocity is generally relative to

the body length, the absolute velocity for a macroscopic motor is larger than that for a microscopic motor. In conclusion, the driving force for a motor in milli-/centimeter is several orders larger than that for a motor in nano-/micrometer.

SI Appendix 7: The mechanism of the autonomous motion of liquid metal motor

According to the experiments, there are some bubbles departing from the liquid metal, which can generate an opposite force to thrust the liquid metal forward. The bubble recoil facilitates the motion. The addition of Al breaks up the symmetry of the liquid metal, which further facilitates the motion in two aspects (Movie S11). On the one hand, according to Rebinder's effect, liquid metal EGaIn or Galinstan would penetrate into aluminum, destroying the oxide skin on Al surface and leading to the activation of Al [3]. The activation of Al makes it react with hydroxide ions more rapidly and efficiently. Such reaction results in the electro-migration of hydroxide ions in the electrical double layer and the electro-osmotic flow of water molecules [4], which generate a momentum equivalent to the water motion. On the other hand, the distribution of the charges across the EDL is altered and a potential gradient is generated along the liquid metal surface, which induces an imbalance of the surface tension on the liquid metal and actuates the metal droplet. Unlike the previously investigated case where external electricity is applied, the electricity in the present system is supplied by the electronegativity property of the Al-liquid metal, and the internal electricity driven motion is more efficient, since the voltage is almost entirely applied on the liquid metal itself. But in former case, most of the voltage is in fact loaded on the electrolyte which is rather resistive thus the efficiency is not very high. Both the potential difference and electrical current are increased due to the contact between the Al and the liquid metal, which induces a higher efficiency for bipolar electrochemical reaction.

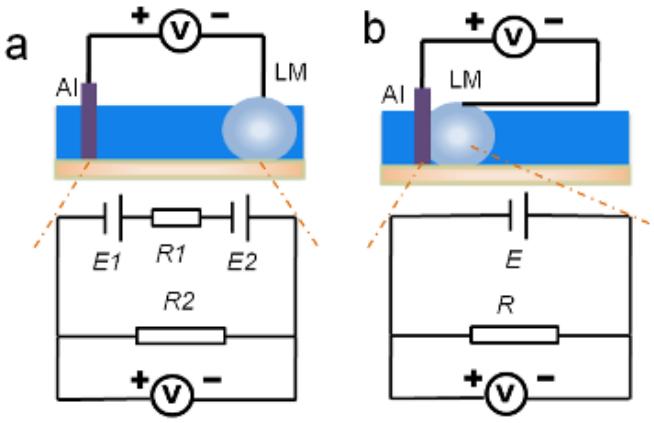

Figure S10. Two different ways to actuate the liquid metal motor. **(a)** The equivalent circuit when the liquid metal is separated from Al. The separation renders an extra resistance *R1* between two metals. **(b)** The equivalent circuit when the liquid metal is contacted with Al. The contact renders the two metals to consist of a galvanic cell, which accelerates the electrochemical reaction.

SI Appendix 8: The pumping effect of an EGaIn motor in a closed-loop open-top channel

For a better demonstration of the pumping effect of the liquid metal motor in a practical device, we further designed and fabricated a closed-loop open-top channel with Poly Lactic Acid (PLA) materials, as shown in **Figure S11**. Such channel is designed by the software SolidWorks2012 and then printed by a 3D printer. The EGaIn mollusk is constrained by the wall of the droplet seat chamber, and the channel contains 0.2 mol/L NaOH solution for reaction. The sphere chamber connects with the channel on its two sides, which consists of the closed loop. Another semicircular chamber is designed to facilitate the addition of the ink. Droplets of ink are added to exhibit the pumping effect. It takes about 22 s to pump the ink for one lap, as shown in Movie S7. More microscopic videos in Movie S8 further provide fluidic details on the pumping effect of the current liquid metal motor. The sectional area of the solution is about 10.28 mm^2, and the overall length of the channel is about 125 mm. Therefore, it can be estimated that the flow rate of such self-powered pump is over 50 mL/s, which is quite high for pumping liquid.

The pumping direction can be altered through stirring the liquid metal motor by a glass capillary, which mainly changes the relative position of the Al attachment. Both clockwise and anticlockwise pumping effects are displayed in the Movie S7.

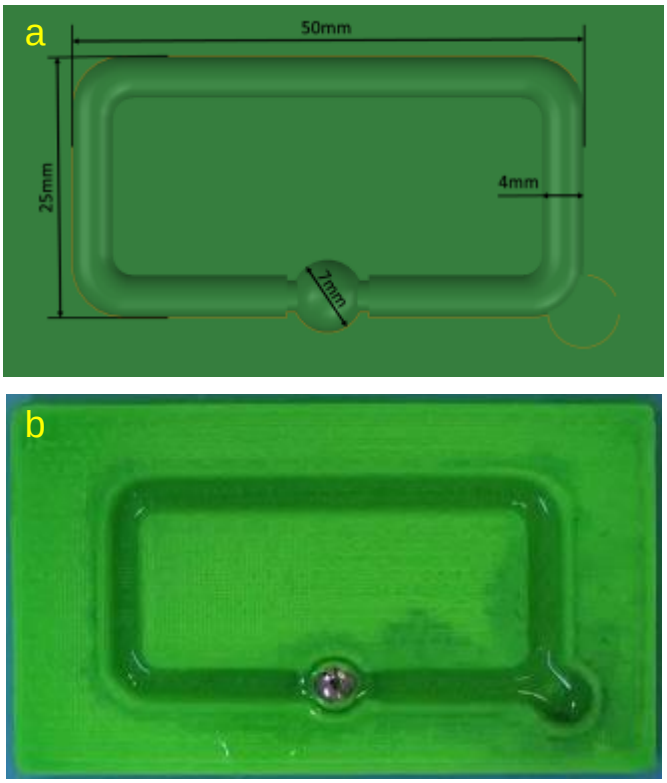

Figure S11. The size and the shape of the printed closed-loop channel. **(a)** The picture is designed by the software SolidWorks 2012. **(b)** This picture refers to the manufactured entity. The 70-μl EGaIn droplet seating in the chamber works as a pump.

SI Appendix 9: The flow field for an EGaIn liquid metal enabled pump

The lateral motion behavior of the current liquid metal motor offers many opportunities for developing future robot machine. One of such typical applications is to directly develop the running sphere as a liquid pump, which should be the first ever self-powered one. A series of experiments were thus performed to demonstrate its role in the fluidic area. Exhibited in **Figure S12** are sequential snapshots for showing the pumping effect of an EGaIn motor with 8 mm width in the PMMA channel containing NaOH solution (0.2mol/L) inside. It can be observed that, when a small bit of Al is fed to the liquid metal, the solution around the liquid metal mollusk flows rather quickly. In order to clearly display such fluidic behavior, a droplet of ink is added to demonstrate the pumping effect and flow field. As it works, the dark ink attenuates in just less than a half second. Depending on an actual need, various pumping velocity can be obtained through justifying the dosage enabled by the liquid metal, the Al and the surrounding solution etc.

Meanwhile, it is noteworthy that in contrast to the nearby flow, the far end flow runs

somewhat different. Two vortexes spin around the liquid metal, while a distant stream flows anticlockwise, as is indicated in **Figure S13** (also shown in Movie S6). This phenomenon may be resulted from the asymmetrical rotational direction of the two vortexes. From the images, it can be found that the ink is dissolved into the solution very quickly. Such effect in fact serves rather well as a new way to induce chaotic advection, which can be utilized to fabricate novel micro-mixer in the near future.

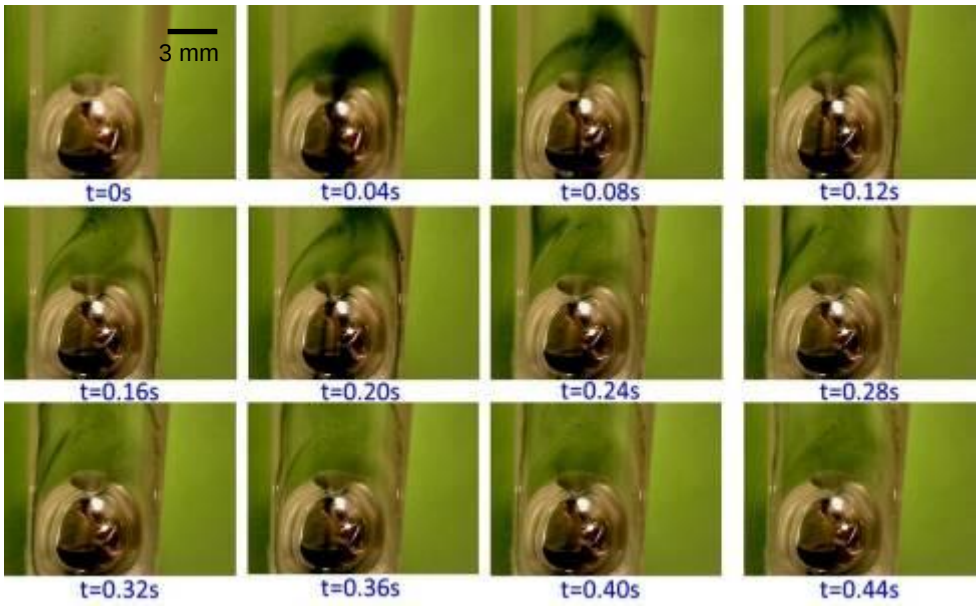

Figure S12. Sequential snapshots for the pumping effect of an EGaIn motor. The volume of the liquid metal is 120 μl, and the concentration of NaOH solution is 0.2 mol/L.

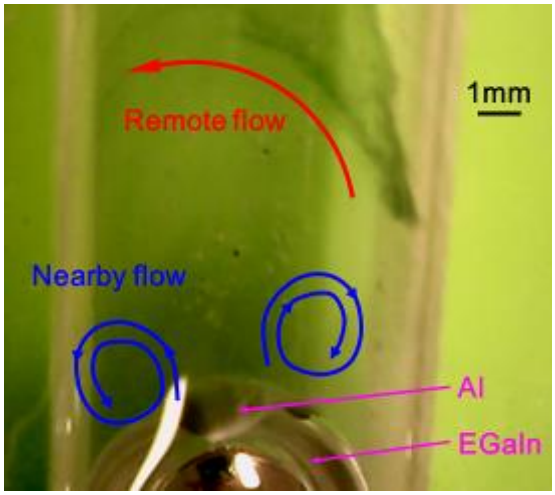

Figure S13. Snapshot for the flow direction of the solution induced by the motion of the liquid metal motor. The volume of the EGaIn motor is 120 μl, and the concentration of NaOH solution is 0.2 mol/L.

Overall, as is shown in the above figures, there are two different parts on the surface of the liquid metal motor: One has a black and dim surface, which refers to the site Al attaching to the liquid metal, while the other part has a polished surface, through which the liquid metal flow can be observed. At the juncture of these two parts, there are some bubbles generated which are soon taken away by the rapid flow.

References:

[1] D. O. Flamini, S. B. Saidman, J. B. Bessone, *Corros. Sci.* **2006**, *48*, 1413.

[2] M. Y. Zhang, S. R. Jing, G. J. Li, Higher Engineering Fluid Dynamics (in Chinese), *Higher Education Press*, **2012**, pp. 302-311.

[3] A. V. Ilyukhina, A. S. Ilyukhin, E. I. Shkolnikov, *Int. J. Hydrogen Energ.* **2012**, *37*, 16382.

[4] Y. Wang, R. M. Hernandez, D. J. Jr Bartlett, J. M. Bingham, T. R. Kline, A. Sen, T. E. Mallouk, *Langmuir* **2009**, *22*, 10451.

Supplementary Movies

Supplementary movies (file attached/ available online)

1. **Movie S1**

   (1) Container: Circular Petri dish made of polystyrene

   (2) Liquid metal volume: 60 μl

   (3) Al dosage: 0.012 g

   (4) Aqueous solution: 0.25 mol/L NaOH

   (5) The metal mollusk moves autonomously along the dish wall with an average velocity of 5 cm/s. The self-propelled motion lasts for more than one hour.

2. **Movie S2**

   (1) Container: A circular open-top channel

   (2) Liquid metal volume: 160 μl

   (3) Al dosage: 0.018 g

   (4) Aqueous solution: 0.25 mol/L NaOH

   (5) The soft metal motor moves autonomously along the circular channel with an average velocity of 1.35 cm/s. The self-propelled motion lasts for more than one hour.

3. **Movie S3**

   (1) Container: A U-shaped open-top channel

   (2) Liquid metal volume: 130 μl

   (3) Al dosage: 0.012 g

   (4) Aqueous solution: 0.25 mol/L NaOH

   (5) The metal motor moves one-way channel with an average velocity of 0.5 cm/s. The velocity fluctuates, which is quicker in the first straight pathway than that in the second.

4. **Movie S4**

   (1) Container: A U-shaped open-top channel

   (2) Liquid metal volume: 170 μl

   (3) Al dosage: 0.012 g

   (4) Aqueous solution: 0.25 mol/L NaOH

   (5) The liquid metal moves back and forth to seek for balance in the U-shaped open-top

channel due to the larger volume of the metal motor.

5. Movie S5

(1) Container: A "zigzag" open-top channel

(2) Liquid metal volume: 150 μl

(3) Al dosage: 0.012 g

(4) Aqueous solution: 0.25 mol/L NaOH

(5) The metal motor moves autonomously along the "zigzag" channel. It can self-adapt its shape at the corner and also squeeze in the narrower pathway.

6. Movie S6

(1) Container: A closed-loop open-top channel

(2) Liquid metal volume: 70 μl

(3) Al dosage: 0.012 g

(4) Aqueous solution: 0.2 mol/L NaOH

(5) This movie is captured by a digital microscope

(6) The bubbles depart from the liquid metal spirally. A drop of ink is added to indicate clearly the flow of the direction.

7. Movie S7

(1) Container: A closed-loop open-top channel

(2) Liquid metal volume: 70 μl

(3) Al dosage: 0.012 g

(4) Aqueous solution: 0.2 mol/L NaOH

(5) The liquid metal pumps the solution counterclockwise and clockwise. A drop of ink is added to indicate clearly the flow of the direction.

8. Movie S8

(1) Container: A closed-loop open-top channel

(2) Liquid metal volume: 70 μl

(3) Al dosage: 0.012 g

(4) Aqueous solution: 0.2 mol/L NaOH

(5) This movie is captured by a digital microscope

(6) The liquid metal pumps the solution clockwise. A drop of ink is added to indicate clearly the flow of the direction.

9. Movie S9

(1) Container: A circular open-top channel

(2) Liquid metal volume: 120μl

(3) Al dosage: 0.020 g

(4) Aqueous solution: 0.2 mol/L NaOH

(5) This movie is captured by a digital microscope

(6) The liquid metal induces a flow field around the liquid metal mollusk, and the flow field is shown by tiny bubbles.

10. Movie S10

(1) Container: A closed-loop open-top channel

(2) Liquid metal volume: 70 μl

(3) Al dosage: 0.012 g

(4) Aqueous solution: 0.2 mol/L NaOH

(5) This movie is captured by a digital microscope

(6) The liquid metal pumps the solution clockwise. Nearby flow field and vortex can be observed by digital microscope.

11. Movie S11

(1) Container: A U-shaped open-top channel

(2) Liquid metal volume: 60 μl

(3) Al dosage: 0.012 g

(4) Aqueous solution: 0.2 mol/L NaOH

(5) This movie is captured by a digital microscope

(6) The process of Al dissolving into the EGaIn liquid metal mollusk. Surface reaction process is clearly displayed.

12. Movie S12

(1) Container: A straight channel

(2) Liquid metal volume: 300 μl

(3) Al dosage: 0.01 g (Activated)

(4) Aqueous solution: 0.2 mol/L NaCl, 0.2 mol/L NaOH

(5) EGaIn does not contract when adding NaCl solution, while it contracts from one end to the other end in sequence and forms into a sphere swiftly when adding a piece of activated Al. In contrast, EGaIn contracts slowly when adding NaOH solution. And it only contracts in half length. If attaching a piece of activated Al, it would continue to contract to the end in sequence swiftly until forms into a sphere at last.

13. Movie S13

(1) Container: A circular open-top channel

(2) Liquid metal volume: 140 μl

(3) Al dosage: 0.018 g

(4) Aqueous solution: 0.25 mol/L Na_2CO_3

(5) The metal motor moves autonomously along the circular channel in the beginning, while after several minutes, it slows down obviously, and a layer of white coverings is coated on the surface of the metal.